SHM
Structural Health Monitoring

Wireless Sensor Networks for Strain Monitoring during Steel Bridges Launching

R. Chacón,[1,*] F. Guzmán,[2] E. Mirambell,[1] E. Real[1] and E. Oñate[2]

[1]*Construction Engineering Department, C/Jordi Girona 1-3, Edificio C1-Campus Nord, Universitat Politècnica de Catalunya UPC, 08034 Barcelona Spain*
[2]*International Centre for Numerical Methods in Engineering (CIMNE) C/Jordi Girona 1-3, Edificio C1- Campus Nord, Universitat Politècnica de Catalunya UPC, 08034 Barcelona Spain*

In this paper, an experimental test performed on a hybrid steel plate girder was subjected to concentrated loads at the end of an unstiffened panel is presented. This load was intended to produce a typical reaction of the piers while launching steel girders in bridges. In this test, strain measurements were taken with conventional pre-wired gauges as well as with newly developed wirelessly connected strain-measuring system. Both measurements were carefully compared and the accuracy of the developed system was demonstrated. Results were also compared with numerical simulations deployed with FE models and on such a basis; the reliability of the developed wireless system was proven. Finally, suggestions of potential research trends in this area are provided.

Keywords concentrated loads · bridge launching · structural control · wireless sensor networks WSN

1 Introduction

The incremental launching method is particularly suited for the construction of continuous multi-span steel plate girder bridges. It consists of assembling and casting sections of the bridge superstructure in a stationary formwork behind an abutment in order to push a completed section forward with jacks along the bridge axis. During launching, the steel segments must be carefully guided. The process often relies only on procedures aimed to control reactions and excessive displacements.

This construction process implies that the reactions of the piers become moving concentrated loads acting in short lengths of the unstiffened webs assembling the plate girders (Figure 1). During launching, the reactions of the piers are expected to be quite large, particularly when the cantilever reaches its maximum value. Whether the patch load is excessive, it might affect the initial condition of the steel girders either by yielding or instability. It is well-known that any change to the material and/or change of the geometrical properties of the considered system might adversely affect the current and future performance of the structure. If these changes occur during the erection of the bridge, the overall integrity of the bridge might be seriously diminished before the whole structure is at service. Hence, measuring the strain at various locations during this phase of construction is important from the perspective of the designer as well as

*Author to whom correspondence should be addressed.
E-mail: rolando.chacon@upc.edu
Figure 13 appears in color online: http://shm.sagepub.com

Los Angeles, London, New Delhi and Singapore
Vol 8(3): 0195–11
[1475-9217 (200903) 8:3;195–11 10.1177/1475921708100779]

construction safety [1,2]. Strain control during launching is, however, unusual. Administrations are rather aloof towards monitoring structures presenting densely gauged deployments during erection since typically cost and complications are increased.

Presently, efforts on developing short-term strain monitoring are increasing [3,4,5]. These efforts have pinpointed the essential requirements needed to perform cost-effective strain-measuring deployments. Portability, power-supply, ease of operation, ability to collect data continuously from multiple channels at some distance and ability to evaluate data in the field are basic requirements of the system. One of the potential strain-measuring deployments that fulfill the aforementioned requirements is the wireless sensor network (WSN). Wireless technologies represent a cost-effective solution for densely populated large-scaled networks and sensors systems [6–10].

In this paper, a laboratory test intended to produce a pier reaction during launching is described. The performed test includes comparing simultaneous strain measurements between a normal pre-wired system and a newly developed wirelessly connected system. Likewise, results are compared with numerical simulations [11]. In such a basis, the reliability of the developed system is demonstrated. Suggestions for further research are provided at the end of the paper.

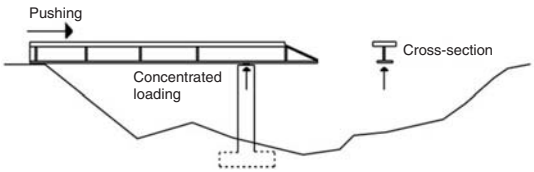

Figure 1 Bridge launching schematic procedure.

2 Review of the Earlier Work

2.1 Concentrated Loads

Concentrated loading upon unstiffened webs might be the most decisive issue when designing a steel bridge that is to be launched. This type of load is commonly referred to as patch loading. A considerable amount of publications as well as state-of-the-art reports dealing with this particular subject can be found on the literature [12–15]. Failure mechanisms as well as critical buckling loads predictions have been proposed throughout the last decades for the case of stiffened and unstiffened panels subjected to compressive concentrated loads. Roughly speaking, it can be stated that the collapse load of plate girders subjected to patch loading depend upon the web slenderness. Stocky webs are prone to fail by yielding whereas slender panels are prone to fail by instability (Figure 2). In either case, the web undergoes folding, whereas the loaded flange a failure mechanism based on plastic hinges. Typically, excessive strain (and thus yielding) is noticed within this web folding at failure.

2.2 Structural Control of Bridges During Launching

The structural control of steel bridges during launching is often performed via reactions and displacements [2]. Reactions are measured throughout the process by stopping the launching for a few hours and placing hydraulic pressure cells in the piers. This is typically performed in critical sections. It is not a continuous measurement though. On the other hand, topographical mea-

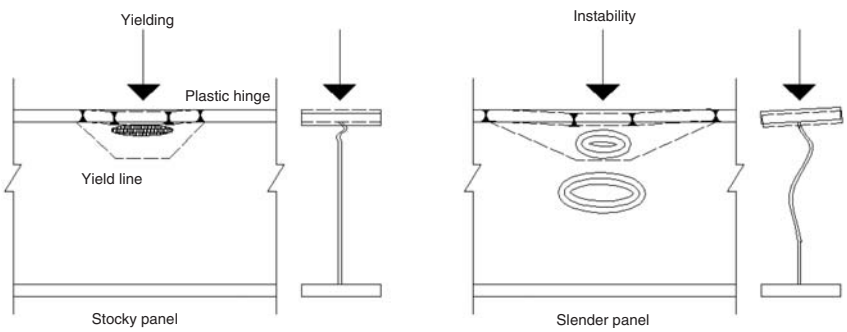

Figure 2 Concentrated loading.

surements are systematically taken from specific points of the whole structure; these latter measurements give a general idea of displacements and deflections, which may warn about potential undesired situations. Temperature changes are also critical and are usually measured. Typically, the lateral displacements are related to these temperature variations. Strain control during launching is, however, unusual. Short-term strain monitoring (e.g., during launching) has been mostly deployed by using fiber optics sensing technology. In particular, the fiber Bragg grating sensors have been demonstrated capable to obtain precise amounts of strain of structures. The utility of FBG sensors has been demonstrated in field applications [3,4] as well as in numerous laboratory tests. Research on structural health monitoring of steel bridges using wireless technology is increasing [16]. Moreover, extensive research has been devoted to wireless sensing technologies [17]. This research is focused on size, power needs and broadcasting capacities of the sensors, which are the basic requirements in structural control with WSN. As these aspects are improved, the systematic usage of this technology can be greatly enhanced.

3 Laboratory Test Description

A test on a steel plate girder intended to produce a concentrated reaction was carried out at the Structural Technology Laboratory of the School of Civil Engineering of Barcelona at UPC. The girder was tested under a static load gradually increased by using displacement control. The load was applied through a 150×200 mm rigid patch load two-dimensionally hinged to a MTS hydraulic jack with a maximum loading capacity of 1000 kN. The steel patch was not fastened to the flange. Laser guides were used on the setting of the girders in the system. Finally, the concentrated load was placed a distance $c = 100$ mm far from the girder end. The girder was tested as simply supported. In both bearings, rotation around the web-plane and movement along the longitudinal axis were allowed. The top flange was laterally restrained for avoiding lateral-torsional buckling failure modes. The test set-up is presented in Figure 3.

The span of the tested girder was 1700 mm, whereas its web height was 700 mm. Three different steel plates were used for the manufacturing of the hybrid girder, the first plate of 4 mm thickness for the web, the second of 20 mm thickness for the flanges, and the third of 20 mm for the stiffeners. Tensile coupon tests were conducted for the purpose of determining the basic stress–strain uniaxial behavior of the material of each plate. Geometrical and statical information is provided in Table 1.

3.1 Instrumentation

Loads, displacements, and strains at key points were measured during the development of

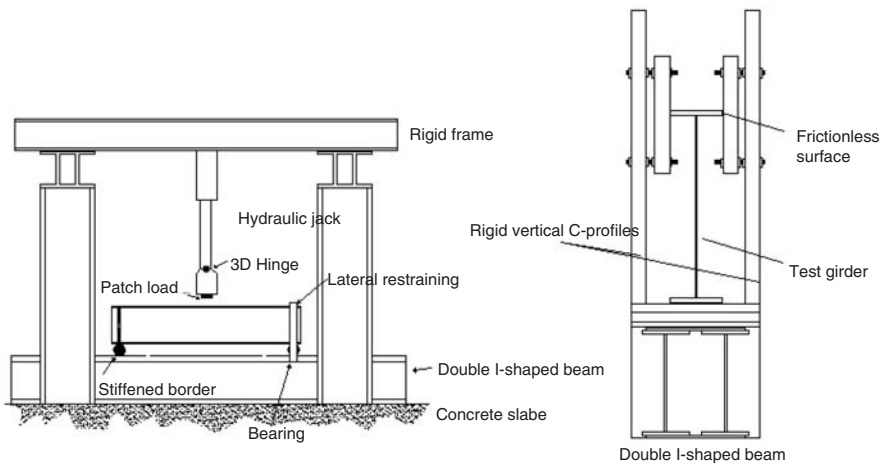

Figure 3 Test set-up in lateral views.

Table 1 Geometrical and mechanical features of the tested girder.

Specimen	l (mm)	h_w (mm)	t_f (mm)	t_w (mm)	t_s (mm)	c (mm)	S_s (mm)	f_{yf} (N/mm^2)	f_{yw} (N/mm^2)	f_{ys} (N/mm^2)
1VEPL	1700	700	20	4	20	100	0	456	325	310

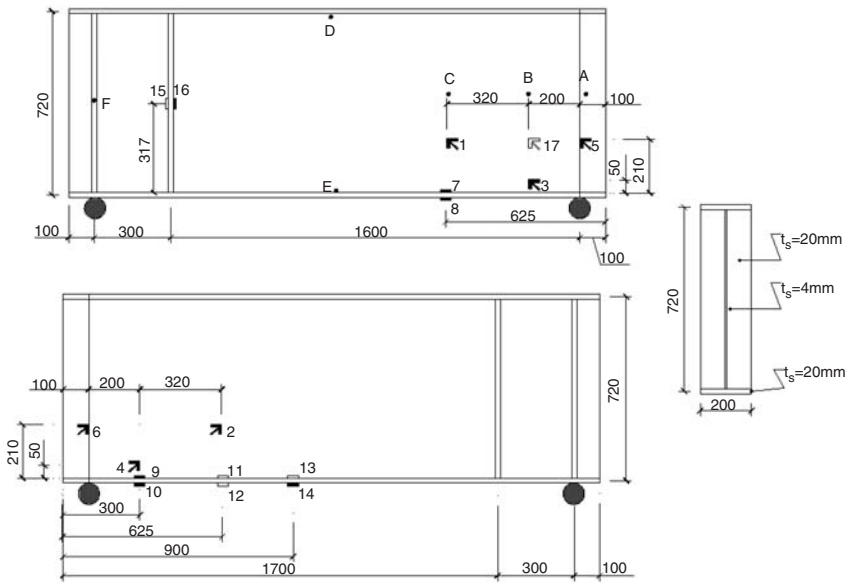

Figure 4 Test instrumentation in opposite views.

the tests. Strain gauges were bonded in zones of the flanges and the web where high stresses were expected to occur. On the other hand, displacements transducers were placed at key determined points of the girders. The measurements were performed with displacement transducers devices ranging from ±50 to ±100 mm. Valuable information about the out-of-plane displacements of the web as well as the vertical displacements of both upper and lower flanges were obtained.

Basically, strain-gauges were located following two criteria; uniaxial gauges were fastened to the flanges (HBM K-RY81-6), whereas triaxial rosettes (HBM K-LY41-6) were fastened in both sides of the thin web. The first group was aimed to capture the development of longitudinal stresses of the bottom flange at different locations, whereas the latter to capture the strain evolution and the potential folding of the web. In both cases, conventional pre-wired gauges (CPG) as well as wirelessly connected gauges (WCG) were bonded. Precise location of all sensors is presented in Figure 4. Table 2 presents useful information related to this figure, in which the principal features of both uniaxial and triaxial gauges as well as the displacement transducers are included.

In order to assess the wirelessly connected system, simultaneous measurements were taken in four different points. The first comparison was performed from gauges 13 (WCG) and 14 (CPG). Secondly, a pair of CPG (7–8) was fastened in such a way that a WCG pair (11–12) was located in the symmetric side of the same flange. Thirdly, an extra comparison was performed on the information obtained from 15 (WCG) and 16 (CPG) in a lowly stressed zone of the transversal stiffener. Finally, a rosette (17) was wirelessly connected (WCG), but no conventional measurements were simultaneously taken. The results obtained with the latter were compared to those obtained with the numerical simulations.

3.2 Data Acquisition System

Two different data acquisition systems (DAS) were employed to collect strain data during the test.

Table 2 Instrumentation chart.

Strain gauges

Sensor	*Symbol*	*Connection*	*Location*	*Resistance (Ω)*	*Gauge factor*	*Transverse sensitivity (%)*	*Maximum strain (%)*
1	↙	Pre-wired	Web	120 ± 0.35	2.06 ± 1%	0.4–0	2
2	↙	Pre-wired	Web	120 ± 0.35	2.06 ± 1%	0.4–0	2
3	↙	Pre-wired	Web	120 ± 0.35	2.06 ± 1%	0.4–0	2
4	↙	Pre-wired	Web	120 ± 0.35	2.06 ± 1%	0.4–0	2
5	↙	Pre-wired	Web	120 ± 0.35	2.06 ± 1%	0.4–0	2
6	↙	Pre-wired	Web	120 ± 0.35	2.06 ± 1%	0.4–0	2
7	–	Pre-wired	Bottom flange	120 ± 0.35	2.05 ± 1%	−0.1	2
8	–	Pre-wired	Bottom flange	120 ± 0.35	2.05 ± 1%	−0.1	2
9	–	Pre-wired	HBM K-LY41-6	120 ± 0.35	2.05 ± 1%	−0.1	2
10	–	Pre-wired	HBM K-LY41-6	120 ± 0.35	2.05 ± 1%	−0.1	2
11	–	Wireless	HBM K-LY41-6	120 ± 0.35	2.05 ± 1%	−0.1	2
12	–	Wireless	HBM K-LY41-6	120 ± 0.35	2.05 ± 1%	−0.1	2
13	–	Wireless	HBM K-LY41-6	120 ± 0.35	2.05 ± 1%	−0.1	2
14	–	Pre-wired	HBM K-LY41-6	120 ± 0.35	2.05 ± 1%	−0.1	2
15	–	Wireless	HBM K-LY41-6	120 ± 0.35	2.05 ± 1%	−0.1	2
16	–	Pre-wired	HBM K-LY41-6	120 ± 0.35	2.05 ± 1%	−0.1	2
17	↙	Wireless	Web	120 ± 0.35	2.06 ± 1%	0.4–0	2

Displacement transducers-Temposonic				Performed comparisons	
Sensor	Symbol	Range	Measurement	Sensors	Location
A	•	±100 mm	Deflection at mid-span (top)	13–14	Bottom flange
B	•	±100 mm	Deflection at mid-span (bottom)	11–7	Bottom flange
C	•	±50 mm	Out-of-plane displacement	12–18	Bottom flange
D	•	±100 mm	Out-of-plane displacement	15–16	Stiffener
E	•	±100 mm	Out-of-plane displacement		
F	•	±50 mm	Bearing movement (control)	17-ABAQUS	Web

3.2.1 Wired System – MGC-Plus (HBM). The MGCplus is a modular computer-controllable measuring amplifier system for universal wired applications. MGCplus has been widely used and benchmarked in different measuring applications and the system performance (24 bits) is judged to lead to high precision. The system allows using quarter, half and full bridge connections. Specific modules have been used throughout the test development. An AP801 module has been used to integrate the LVDT sensors and four AP810 modules has been used to integrate the strain gauges sensors. The results coming from the MGCplus were collected in a database storage format.

3.2.2 Wireless System. MICA2-MDA300 (Crossbow). The second DAS is innovatively wirelessly connected. It is provided by Crossbow technology, Inc [18] and the entire system is referred to as a WSN platform. WSNs are represented by nodes; each node is able to integrate sensors, perform local processing, and communicate the information wirelessly to a base station. Mica2-like motes (Figure 5(a)) have been used as nodes throughout the test. These devices integrate a control unit directed by means of an AtMega128L microprocessor and a 916 MHz radio frequency system.

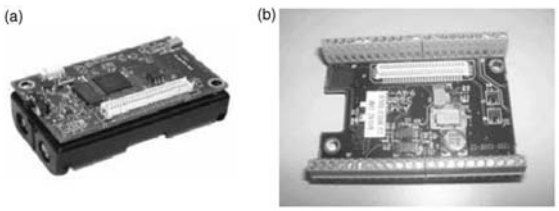

Figure 5 (a) Mica2-like mote. (b) MDA300 [18].

The coming signal from the strain gauge sensor must be converted to a digital signal. In this particular case, a MDA300 board (Figure 5(b))

has been used. This card presents a 12 bits analogue-to-digital converter. Input capacity of the board ranges dynamically from 0 to 2.5 V. It is widely known that gauges measure strain as a function of their resistance variance. As the material deforms, the gauge-foil is also deformed, causing the resistance of the wire to change as it is stretched. This resistance change can be measured using a Wheatstone bridge. The signal is then amplified and finally filtered with a low pass filter before it is sent to the analog-to-digital converter.

The Wheatstone bridge is integrated by 120 Ohms, 1%-tolerant resistances. Furthermore, an AD620B amplifier was used within the circuit. The gain was adjusted to generate an output ranging from 0 to 2.5 V from the sensor signal in order to fit with the analogue-to-digital converter. A reference voltage was set to 1.25 V in the amplifier; in this way the initial cero value of the strain gauge is moved to 1.25 V in order to measure both tensile- and compressive-based signals. The 1.25 V value was selected because is the middle point of the full scale value from the analogue to digital converter, in this way we can measure compressive values from 1.25 to 0 V; and tensile values from 1.25 to 2.5 V. The low pass filter was implemented to cut-off all frequencies above 10 Hz. The objective is to eliminate the signal-noise due to high frequencies. The 10 Hz value has been selected due to the magnitude of the measured low-frequency signals. The wired system has a similar filter. In this case the circuit is integrated within the structure of the global device. Both systems have the same function and as a result, both magnitudes can be compared (Figure 6).

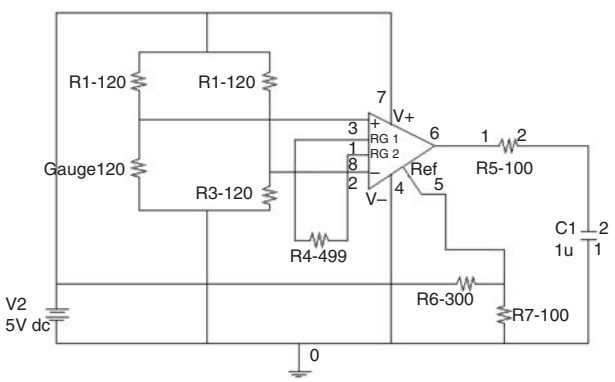

Figure 6 Signal conditioning circuit.

A total of seven strain gauge sensors were distributed in five Mica2 motes. Four Mica2 motes measured uniaxial strain (labeled as 11, 12, 13, and 15 in Table 2) with one single sensor each, whereas one Mica2 measured strain in three different axes (labeled as 17 in Table 2). Power was supplied by four C-1.5 V alkaline batteries, offering a total of 6 V. The voltage was regulated to 3 V for the sake of keeping it constant and increasing the system autonomy. Measured data were wirelessly sent to a base station connected to the USB port in a personal computer. Once stored, the information was readily interpreted from typical text files.

4 Numerical Model

The numerical model implemented in the multi-purpose code ABAQUS, which includes geometrical and material nonlinearities was used as a control tool. The experimental test was numerically reproduced in accordance with the European guidelines EN1993-1-5-Annex C (FE-analyses) [19]. An incremental nonlinear analysis was performed by using a Riks algorithm on an initially perturbed geometry with an elastic plastic constitutive equation. The reproduction of the test was based upon the following characteristics: the initial imperfection of the girder was assumed as being related to the first eigenmode of the girders (Figure 7), the adopted scale was related

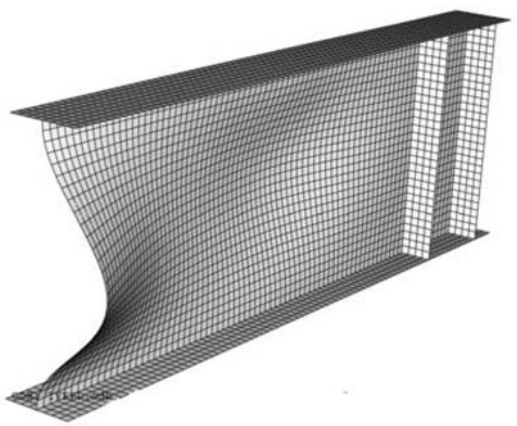

Figure 7 First critical eigenmode of the girder subjected to concentrated load.

to fabrication tolerances as recommended by [19], the elastic-plastic constitutive equation was taken from tensile coupons tests performed from the plates, realistic boundary conditions were included; i.e, the girder was entirely modeled as simply supported with a restrained flange and finally, a typical pattern of residual stresses in welded girders was included as initial structural conditions in the analysis. S4 shell elements provided in ABAQUS libraries were employed in the modeling.

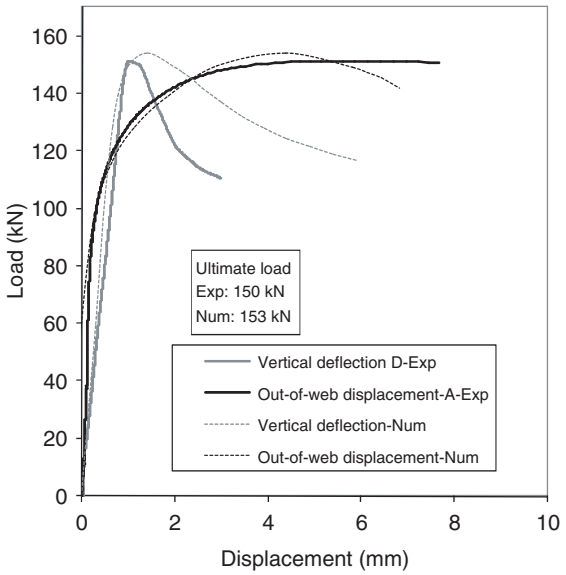

Figure 8 Experimental and numerical results.

5 Results

The general response of the girder when subjected to a concentrated load at the end of the panel is characterized in Figure 8. Two types of displacements measured throughout the test are plotted against the applied load. The vertical displacement at the end of the girder as well as the out-of-plane displacement of the web panel are plotted from results obtained experimentally (continuous lines) and numerically (dashed lines).

Numerical results are judged to be accurate. Pre-peak branches match quite precisely and ultimate load results numerically obtained coincided very well with the experimental values. There are some discrepancies in the post-peak branch for the load-vertical deflection plot. In this range, however, the out-of-web response is well reproduced. The failure mode is displayed in Figure 9. This figure includes experimentally and numerically obtained isometric views. Web folding as well as flange sagging are noticeable. The numerical model reproduces satisfactorily the experimental observations.

Figure 10 shows schematically the failure mode as well as the location of the strain measurements. It is observed that the pairs of gauges 9–10, 12—8, and 11–7 are located fairly close to the sagged area of the flange. Moreover, the pair of gauges 13–14 was fastened far from

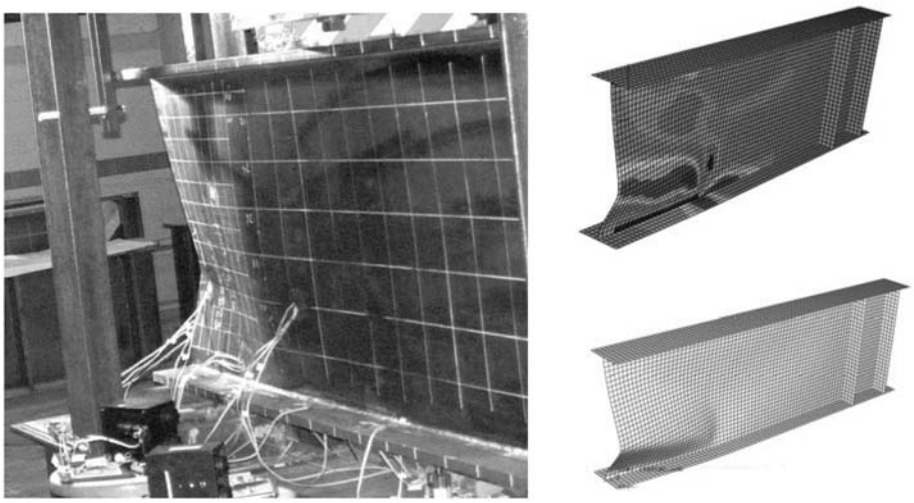

Figure 9 Experimental and numerical results.

this zone. This fact is critical and may explain the results presented in the forthcoming.

5.1 Pre-wired Versus Wireless Results

Firstly, pairs of gauges 12–8 and 11–7 were analyzed. These gauges were symmetrically located at both sides of the flange as shown in Figure 4 and 10. Microstrain-versus-time plots are sketched in Figure 11(a) for gauges 12–8 and in Figure 11(b) for gauges 11–7. The gauges of pair 12–8 were fastened on the bottom side of the flange thickness, whereas the gauges of pair 11–7 were fastened on the upper side of the flange. These gauges were fastened nearby the sagged area of the flange (theoretically, the plastic hinge). Results show that linear branches are quite similar. Subsequently, both gauges detect the lost of linearity due to instability and/or yielding. Once the collapse load occurs and the hinge is formed, the longitudinal strain might vary through the flange thickness. Probably due to local phenomena occurring on this zone, the post peak branches differ from one gauge to another. Symmetry is not observable from this point onwards. Tensile stresses are observed during the whole analysis at this location.

Figure 12 shows a comparison between the gauges 13 and 14, which were fastened one opposite to another. These gauges were not fastened close to the sagging zone. The trends as well as the strain values practically coincide in both linear and post-peak branches. In this case, the lost of linearity is also detected in both cases. Uniform tensile stresses are observed during the whole analysis at this location. Symmetry in straining at both sides of the flange is observable in this case.

If CPG gauges 9–10 are plotted in the same fashion (Figure 13), a rather different trend is observed.

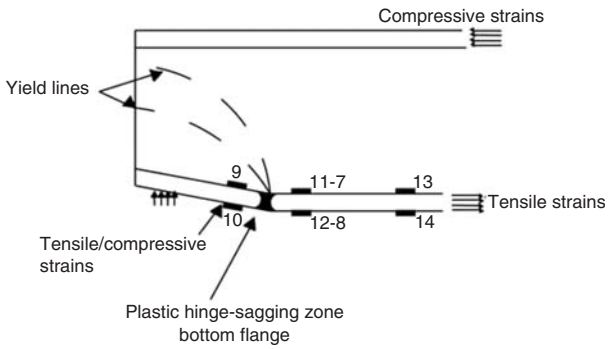

Figure 10 Schematic failure mode.

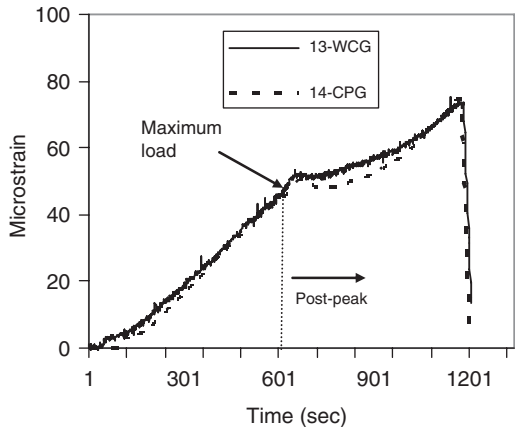

Figure 12 Microstrain vs time for pair of gauges 13–14.

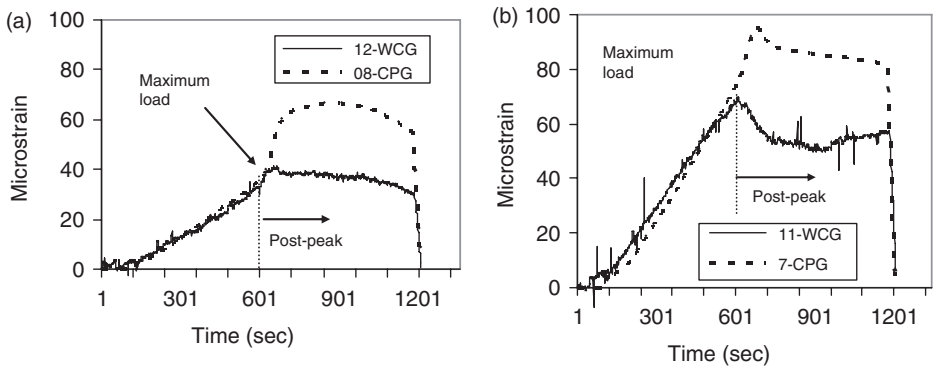

Figure 11 Microstrain vs time plot for pairs of gauges 12–8 (a) and 11–7 (b).

Compressive strains develop in the upper side of the thickness of the bottom flange in the post-peak branch. The one-hinge failure mechanism depicted in Figure 10 may be the key for understanding the observed phenomena. When the plastic hinge is developed, the bottom flange presents a bending-like behavior. If gauges are located within this zone, longitudinal strains are prone to present opposite signs at both sides of the flange thickness. In either case, the lost of linearity is noticeable.

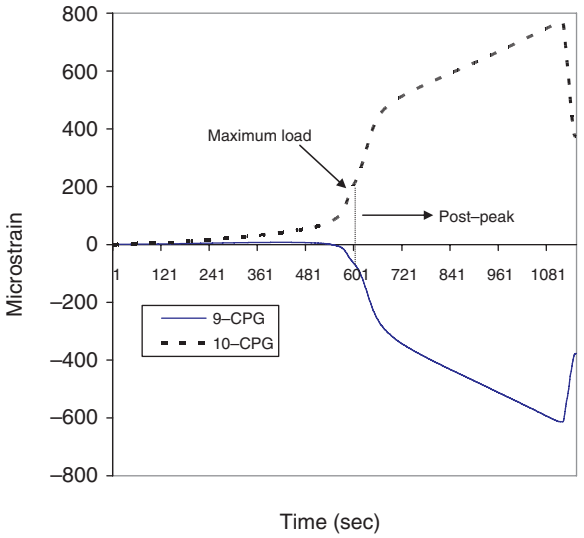

Figure 13 Microstrain vs time for pair of gauges 9–10.

5.2 Numerical versus Wireless Results

Finally, strains measurements obtained with rosette WCG-17 are provided. Likewise, strains obtained with the numerical model are used. WCG-17 gives valuable information about strains at one side of the web plate. The state of strain at a point of a material is defined if the direct strains, ε_x, ε_y, and an additional direction are known (in this case, ε_{45°). For the sake of comparison, two plots are sketched in Figure 14. The first plot (Figure 14(a)) relates the applied load versus the first invariant of strain (which states that the sum of two perpendicular normal strains is a constant). This invariant is calculated from ε_x and ε_y in both experimental (WCG) and numerical results. Accuracy of the obtained results is satisfactory. The trend is well reproduced with the numerical model and values coincide quite well. Secondly, WCG-ε_{45° strains are compared to those obtained with the numerical model in Figure 14(b), in which a quite similar response is observed.

5.3 Proposals for structural control

The depicted wireless strain-measuring system may be suitable for control purposes during bridge launching. Precautions before yielding can be given if the strain attains unacceptable levels.

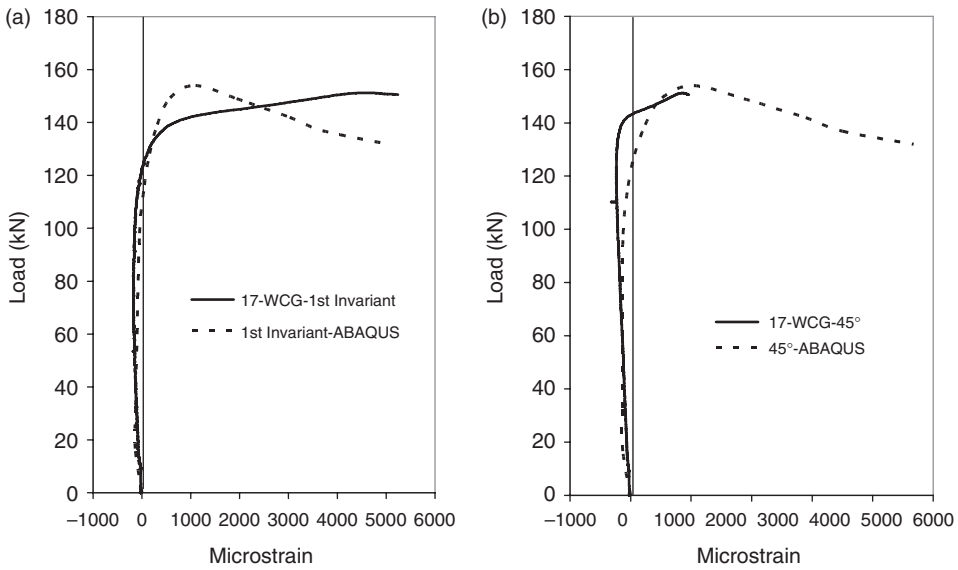

Figure 14 (a) Load vs first strain invariant, (b) Load vs ε_{45°.

In addition, anomalies related to unexpected lost of linearity of the system can be inferred from the responses obtained with the measurements. For the sake of demonstrating these capabilities, microstrain-versus-time plots are displayed as potential control tools.

Figure 15 shows the evolution of the maximum principal strain of WCG-17 throughout the test. In this case, the yielding criterion is defined in such a way that whether the maximum principal strain exceeds a certain value (namely, $\varepsilon_{\max} \geq f_{yw}/E$), the web is said to yield. Thus, the maximum allowable value of microstrain ($\sim$1550 $\mu\varepsilon$ for the steel of the web plate of the tested girder) can be indicated with a horizontal line. If bridge girders that are to be launched shall be designed to avoid unacceptable damage, the measured strain values must not exceed the defined bounds. In a real structure, this type of plots may warn whether the structure is attaining high strain levels. In addition, an eventual unexpected lost of linearity can be noticed within the progressive measurement.

In Figure 15, it is observed that as the load is statically increased, the principal strain is also increased, but it does not reach the maximum allowable value of microstrain. When the load seizes a certain level, the linearity is lost and the strain-levels go far beyond this limit. It is worth bearing in mind that the test was performed under displacement control to values that exceeded considerably the collapse load. Accordingly, significant plastic strain was measured by WCG-17. Real launched should not attain this value.

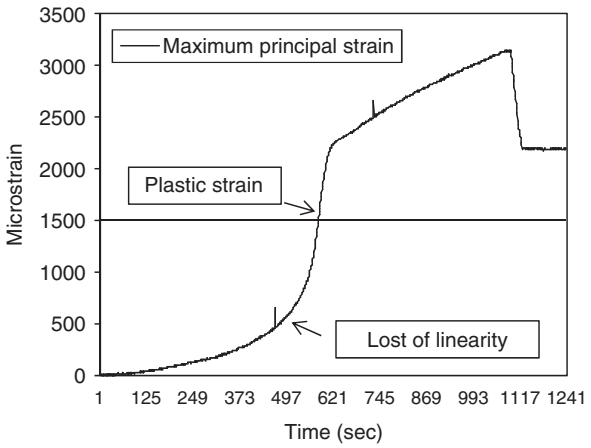

Figure 15 Proposed plots for structural control.

Eventually, as the static system is varied during launching (first the girder behaves as a cantilever and then as a multi-span continuous beam), the curve can increase and/or decrease gradually.

It is, however, recognized that the structural health monitoring of steel girders during bridge launching requires a vast amount of sensors and thus, simultaneous measurements. The system described here monitors the structural integrity of steel girders during launching for only one measure point. Graphical user interfaces (GUI) and database management systems should be required for large WSN deployments. The usage of these technologies together with the upcoming improvements of the sensors on power supply, lightness, and ease of operation would allow for the systematic deployment of the described technology.

6 Conclusions

A wirelessly connected measuring system is presented and assessed by means of a half-scale test deployed on a hybrid steel plate girder loaded up to failure. This newly developed measuring system may be particularly suited for controlling excessive straining of web girders in steel bridges during launching and/or detecting any change of the girder properties. For the sake of assessing the reliability of the newly developed WSN system, a number of comparisons were performed upon conventionally pre-wired gauges, wireless sensors, and numerical simulations. First, strains obtained with the wirelessly connected gauges WCG were compared to the conventionally prewired CPG measured values. Second, the WCG measurements were compared to those obtained with numerical simulations. The results obtained were judged to be satisfactory for the former and the latter. Thus, the reliability of the system was proven.

Finally, it is shown how the depicted wireless strain-measuring system may be suitable for control purposes during bridge launching. Precautions before yielding and/or any change of the system can be pinpointed from plots that indicate when high levels of strain are attained and/or eventual anomalies in the linearity occur. Numerical tools may be also used for further control of the system.

The proposed technology may not be limited to monitoring during bridge launching but additionally, for on-site continuous bridge performance and condition monitoring. The long-term performance of the sensors may be suitable whether the actual power supply and remote data acquisition technologies are enhanced. Recognizably, further research on practical application of large WSN is needed.

Acknowledgments

The authors wish to gratefully acknowledge the financial support provided by Spanish Ministry of Science and Education, as a part of the Research Project BIA 2004-04673 as well as a part of the PROFIT Project PROSENSOR CIT 380000-2005-16. Likewise, the authors are grateful to Arcelor and Tadarsa for supplying and manufacturing the girders. Finally, the first author wish to acknowledge the grant provided within the research project.

References

1. Vohra, S., Johnson, G., Todd, M., Danver, B. and Althouse, B. (1999). Strain Monitoring during Construction of a Steel-box Girder Bridge with Arrays of Fiber Gragg Sensing Sensors, Internal Report Naval Research Laboratory, NRL/MR/5670-99-8390.
2. Lebet, J.P. (2004). *Measurements Taken During the Launch of the 130 m Span Vaux Viaduct*, In: Proceedings, International Symposium of Steel bridges 23 24, June, Millau, France: Steelbridge, OTUA.
3. DeWolf, J., Lauzon, R. and Culmo, M. (2002). Monitoring bridge performance. *Structural Health Monitoring*, *1*, 129.
4. Shehata, E. and Rizkall, S. (1999) Intelligent sensing for innovative bridges. *Journal of Intelligent Material Systems and Structures*, *10*, 304. (DOI: 10.1177/1045389X9901000406)
5. DeWolf, J.T. (2006) *The Long Term Structural Health Monitoring of Bridges in the State of Connecticut*, Granada, Spain: Third European Workshop on Structural Health Monitoring.
6. Culler, D. and Hong, W. (2004). Wireless sensor networks. *Communications of the ACM*, *47*, 30–33.
7. Lynch, J. (2007). An overview of wireless structural health monitoring for civil structures. *Philosophical Transactions of the Royal Society Academy*, *365*, 345–372. (DOI: 10.1098/rsta.2066.1932)
8. Glaser, S. (2004). Some real-world applications of wireless sensor nodes. In: *Proceedings of the 11th Annual International Symposium on Smart Structures and Materials. SPIE—International Society for Optical Engineering*, Vol. 5391, pp. 344–335, San Diego, CA, USA.
9. Chee-Yee, C. and Kumar, P. (2003). Sensor networks: evolution, opportunities and challenges. In: *Proceedings of the IEEE*, *91*(8), 1247–1256.
10. Farhey, D. (2006). Integrated virtual instrumentation and wireless monitoring for infrastructure diagnostics. *Structural Health Monitoring*, *5*, 29. (DOI: 10.1177/1475921706057980)
11. ABAQUS, 6.5 Version. (2005). Manuals, Abaqus Inc.
12. Lagerqvist, O. and Johansson, B. (1996) Resistance of I-girders to concentrated loads. *Journal of Constructional Steel Research*, *39*(2), 87–119.
13. Graciano, C. and Johansson, B. (2003). Resistance of longitudinally stiffened I-girders subjected to concentrated loads. *Journal of Constructional Steel Research*, *59*(5), 561–586.
14. Markovic, N. and Hajdin, N. (1992). A contribution to the analysis of the behavior of plate girders subjected to patch loading. *Journal of Constructional Steel Research*, *21*, 163–173.
15. Elgaaly, M. (1983). Web design under compressive edge loads. *Engineering Journal*, *20*(4), 153–171.
16. Rong, A.Y. and Cuffari, M.A. (2004). Structural healthmonitoring of a steel bridge using wireless strain gauges. *Structural Materials Technology VI*, pp. 327–330, Buffalo, NY: NDE/NDT for Highways & Bridges.
17. Lynch, J. and Loh, K. (2006). A summary review of wireless sensors and sensor networks for structural health monitoring. *The Shock and Vibration Digest*, *38*, pp. 91–128. (DOI: 10.1177/0583102406061499)
18. Crossbow Technology, Inc. MTS/MDA Sensor Board User's Manual. Crossbow, Inc. (www.xbow.com)
19. EN 1993-1-5. (2005). Eurocode 3: Design of steel structures, Part 1.5 "Plated structural elements".